Unconventional superconductivity on the triangular lattice Hubbard model

Kuang Shing Chen,[1,*] Zi Yang Meng,[1,2,†] Unjong Yu,[3] Shuxiang Yang,[1,2] Mark Jarrell,[1,2] and Juana Moreno[1,2]

[1] *Department of Physics and Astronomy, Louisiana State University, Baton Rouge, LA 70803, USA*
[2] *Center for Computation and Technology, Louisiana State University, Baton Rouge, LA 70803, USA*
[3] *GIST-College, Gwangju Institute of Science and Technology, Gwangju 500-712, Korea*

Using large-scale dynamical cluster quantum Monte Carlo simulations, we explore the unconventional superconductivity in the hole-doped Hubbard model on the triangular lattice. Due to the interplay of electronic correlations, geometric frustration, and Fermi surface topology, we find a doubly degenerate singlet pairing state at an interaction strength close to the bare bandwidth. Such an unconventional superconducting state is mediated by antiferromagnetic spin fluctuations along the Γ-K direction, where the Fermi surface is nested. An exact decomposition of the irreducible particle-particle vertex further confirms the dominant component of the effective pairing interaction comes from the spin channel. Our findings provide support for chiral $d+id$ superconductivity in water-intercalated sodium cobaltates $Na_xCoO_2 \cdot yH_2O$, as well as insight into the superconducting phases of the organic compounds κ-$(ET)_2X$ and $Pd(dmit)_2$.

PACS numbers: 71.27.+a, 71.10.Fd, 74.20.Rp, 74.70.-b,

Introduction.- Since the discovery of the Cu-based high temperature superconductors, the search for new unconventional superconductors is among the central topics in condensed-matter physics [1]. The water-intercalated sodium cobaltates $Na_xCoO_2{\cdot}yH_2O$ [2–4] and two families of organic charge-transfer salts κ-$(ET)_2X$ and $Pd(dmit)_2$ [5–10] are of particular interest. The underlying structure of these layered materials is the geometrically frustrated triangular lattice. The competition between electronic correlations and geometric frustration yields novel phenomena. For example, the most frustrated members of the κ-$(ET)_2X$ and $Pd(dmit)_2$ families are believed to host quantum spin liquid states [11], and the recently discovered 5K superconducting phase in $Na_xCoO_2.yH_2O$ might be a chiral state which breaks parity and time reversal giving rise to interesting edge modes that can carry quantized particle and spin currents [12–14].

The layered triangular lattice compound $Na_xCoO_2 \cdot yH_2O$ has a superconducting dome for $x \sim 0.3$, $y \sim 1.3$ at $T_c \sim 5$ K [2–4]. Due to intercalation, its electronic structure is effectively two-dimensional. A very rich phase diagram has been mapped out for a range of Na concentrations [4]; however, the nature of the superconducting phase has remained poorly understood. Recent measurements on high quality single crystals [15] show that the spin contributions to the Knight shift decreases below T_c along the a and c axes, supporting the notion that the Cooper pairs are formed in a spin-singlet state. The temperature and doping dependence of the Knight shift and the relaxation rate above T_c provide evidence of antiferromagnetic correlations [15, 16].

There are a number of theoretical proposals for the unconventional superconductivity in the cobaltates. The underlying triangular lattice allows a doubly degenerate E_2 representation of the superconducting order parameter with $d_{x^2-y^2}$ and d_{xy} degenerate states [1, 13, 17], raising the exciting possibility of a time-reversal symmetry breaking chiral $d_{x^2-y^2} \pm id_{xy}$ superconductor. Earlier studies of the cobaltates draw analogy to the cuprates and employed either a phenomenological RVB theory [18], or a slave boson mean-field approach [19] to provide signatures of a spin-singlet $d+id$ pairing state. Recent studies of the sodium cobaltates using a Gutzwiller projection supplemented by symmetry arguments [12], as well as the multi-orbital functional renormalization group [14], reveal a rich phase diagram with an anisotropic $d+id$ phase and a possible topological quantum phase transition through a nodal superconducting state. However, prior approaches suffer either from their mean-field nature, or their incapability of capturing correlation effects in the strong coupling regime. Hence, there is an urgent need of unbiased studies, where the interplay of strong electronic correlations and geometric frustration can be treated in a non-perturbed fashion.

The simplest model that captures the essential physics of the cobaltates is the single-band Hubbard model on a triangular lattice. In this Letter, we explore the low-energy properties of this model by large-scale dynamical cluster quantum Monte Carlo simulations [20]. We focus on the different superconducting instabilities in the hole-doped side of the phase diagram. To the best of our knowledge, this is the first study of the hole-doped Hubbard model on the triangular lattice exploring the pairing symmetries on different cluster sizes. Clusters up to size $N_c = 12$ allow a greater momentum resolution and higher quality data on the spectral function, self energy, and different superconducting susceptibilities. Therefore, we obtain an unambiguous signature of an unconventional doubly-degenerate superconducting state in the strong to intermediate coupling region. By explicitly comparing the pairing susceptibility in the s-, $d_{x^2-y^2}$-, d_{xy}-wave singlet channels and the f-wave triplet channel, we find that the $d_{x^2-y^2}$ and d_{xy} components are

most divergent and extrapolate to the same T_c within our numerical accuracy. We identify that the pairing is mediated by strong spin fluctuations along the antiferromagnetically (AF) ordered wavevector on the Γ to K direction. The Fermi surface (FS) is nested along this AF wavevector, but the system only orders at half-filling in the Heisenberg limit. An exact decomposition of the irreducible particle-particle vertex furthermore reveals the dominant part in the effective pairing interaction comes from the spin channel.

Formalism.- The Hamiltonian of the system is $H = \sum_{\mathbf{k}\sigma} \epsilon^0_{\mathbf{k}} c^\dagger_{\mathbf{k}\sigma} c_{\mathbf{k}\sigma} + U \sum_i n_{i\uparrow} n_{i\downarrow}$, where $c^\dagger_{\mathbf{k}\sigma}(c_{\mathbf{k}\sigma})$ is the creation (annihilation) operator for electrons with momentum $\mathbf{k}$ and spin σ, $n_{i\sigma} = c^\dagger_{i\sigma} c_{i\sigma}$ is the number operator, and the bare dispersion is given by $\epsilon^0_{\mathbf{k}} = -2t\cos(k_x) - 4t\cos(\sqrt{3}k_y/2)\cos(k_x/2)$ with t being the hopping amplitude between nearest neighbor sites, and U the on-site Coulomb repulsion.

We investigate one and two-particle properties of the model using the dynamical cluster approximation (DCA) [21] with weak-coupling continuous time quantum Monte Carlo (CTQMC) [22] as the cluster solver. The DCA maps the original lattice onto a periodic cluster of size N_c embedded in a self-consistently determined host. Spatial correlations inside a cluster are treated explicitly while those at longer length scales are described at the mean-field level. In this work we choose clusters of sizes $N_c = 4, 6, 8$ and 12. We study inverse temperatures up to $\beta t = 16.5$. We obtain the cluster self-energy $\Sigma(\mathbf{K}, \omega)$ via the maximum entropy method [23] (MEM) applied directly to the Matsubara-frequency self energies calculated by the DCA-CTQMC [24, 25]. We then interpolate the $\Sigma(\mathbf{K}, \omega)$ to obtain the lattice self energy, $\Sigma(\mathbf{k}, \omega)$, and lattice spectral function, $A(\mathbf{k}, \omega)$.

To obtain various susceptibilities, $\chi(T)$, we extract the irreducible vertex function Γ via the Bethe-Salpeter equation from the two-particle Green function measured on the cluster, then employing $\chi(T) = \dfrac{\chi_0}{1 - \Gamma\chi_0}$, where χ_0 is the bare susceptibility constructed from the dressed one-particle lattice Green function. The superconducting pairing susceptibilities are obtained from the particle-particle channel, and the charge and spin susceptibilities are obtained from the particle-hole channel. We further separate the pairing susceptibilities explicitly into spin singlet and triplet channels, where in the singlet channel we project the $\chi(T)_{pairing}$ onto s-, $d_{x^2-y^2}$-, and d_{xy}-wave, and in the triplet channel we project it onto the f-wave channel, with the corresponding form factors [1, 14].

To explore the pairing mechanism we decompose the particle-particle pairing vertex Γ into the fully irreducible vertex Λ, the charge ($S = 0$) particle-hole contribution, Φ_c, and the spin ($S = 1$) particle-hole contribution, Φ_s, through the parquet equation, $\Gamma = \Lambda + \Phi_c + \Phi_s$ [26]. We furthermore project the previous expression using different form factors such as $d_{x^2-y^2}$ and d_{xy},

$$V_{d_{x^2-y^2}/d_{xy}} = V^{\Lambda}_{d_{x^2-y^2}/d_{xy}} + V^{C}_{d_{x^2-y^2}/d_{xy}} + V^{S}_{d_{x^2-y^2}/d_{xy}}, \quad (1)$$

where each term is the projected component of the corresponding term in the parquet equation [27]. In this way, we are able to distinguish which component contributes the most to the effective pairing interaction.

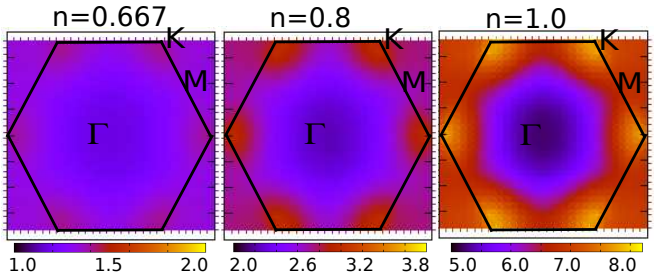

FIG. 1: (Color online) Cluster spin susceptibility for $N_c = 12$, interaction strength $U = 8.5t$, temperature $T = 0.1t$ and different fillings, $n = 0.667$, 0.8, and 1.

Results.- Fig. 1 displays the cluster spin susceptibility at different fillings, $n = 0.667$, 0.8, and 1, and coupling $U = 8.5t$. The data are obtained from DCA-CTQMC simulations with cluster size $N_c = 12$, and we interpolate the cluster susceptibility into the entire Brillouin zone (BZ). At very high hole-doping, $n = 0.667$, the susceptibility is mostly flat. As the filling increases, $n = 0.8$, the spin susceptibility develops six bumps at the K points. When $n = 1$, the bumps become more pronounced. The vector connecting Γ to K is the antiferromagnetically ordered wave vector ($\mathbf{Q_{AF}}$) in the Heisenberg limit of the half-filled model. The cluster spin susceptibility demonstrates that the antiferromagnetic fluctuations become stronger as the filling moves towards $n = 1$. The pairing of electrons may be mediated by these fluctuations [28, 29].

Fig. 2 shows the Fermi surface (FS) at the same fillings used in the previous figure. Fig. 2 (a) corresponds to the non-interacting limit. At $n = 0.667$, 0.8 and 1 the FS is close to a perfect circle. The van Hove singularity in the non-interacting band structure is present at $n = 1.5$ with saddle points at M. One-loop RG calculations [30] show the FS in the hole-doped side is stable against weak Coulomb interactions. However, under strong interaction, the FS begins to deform. Fig. 2 (b) displays the FS at $n = 0.667$, $U = 8.5t$, which is slightly deformed towards a hexagon. The red arrow corresponds to $\mathbf{Q_{AF}}$, while the pink arrow is this vector shifting its center to Γ and rotating it by 60^o. For $n = 0.667$ the pink arrow is longer than the diameter of the FS so there is no nesting effect, and we do not observe superconductivity at this filling. In Fig. 2 (c), $n = 0.8$, the FS is more deformed, the $\mathbf{Q_{AF}}$ now connects significant sections of the FS, and as illustrated in Fig. 1, the AF fluctuations

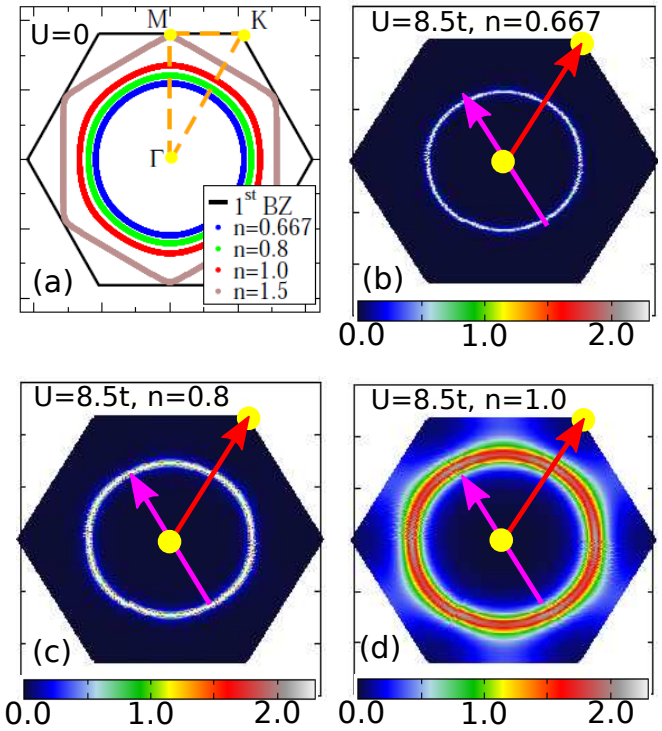

FIG. 2: (Color online) (a) First Brillouin zone, the symmetric path $\Gamma - M - K - \Gamma$ and the non-interacting Fermi surface at different band fillings. (b), (c), (d) Spectral function $A(\mathbf{k}, \omega = 0)$ on the Fermi surface for $N_c = 12$ DCA-CTQMC simulations with $U = 8.5t$, $T = 0.1t$, and $n = 0.667$ in (b), $n = 0.8$ in (c), and $n = 1$ in (d). Red arrow is the AF ordered wave vector ($\mathbf{Q_{AF}}$) and the pink arrow is after shifting its center to Γ and rotating it by 60^o.

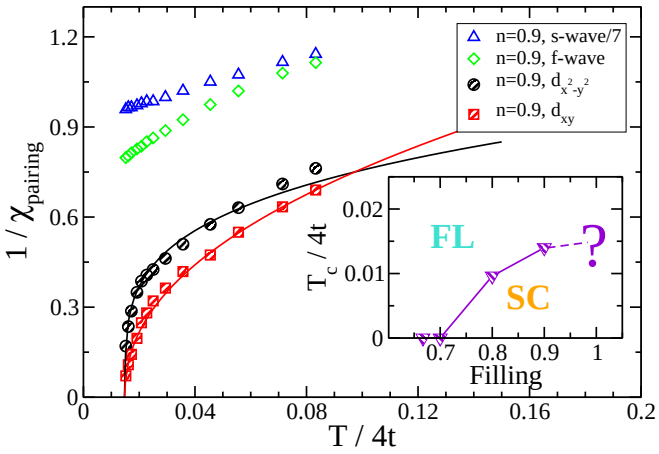

FIG. 3: (Color online) Inverse pairing susceptibility, $1/\chi_{pairing}$, for $N_c = 6$, $U = 8.5t$ and $n = 0.9$. The singlet s-wave and triplet f-wave do not diverge, whereas the singlet pairing channels with $d_{x^2-y^2}$- and d_{xy}-wave symmetry show a divergencency at the same T_c. Note that we have multiplied by a factor of 7 the s-wave pairing susceptibility in order to use the same vertical scale. Inset, the superconducting transition temperature T_c as a function of doping. FL and SC label the Fermi liquid and superconducting regions, respectively.

are stronger. The nesting effect and the strong AF fluctuations together give rise to diverging pairing susceptibilities at filling $n = 0.8$ and 0.9, as discussed below. At half-filling, $n = 1$, the FS is further deformed towards a hexagon, but the spectral weight become less coherent due to the strong interaction. Interestingly, the nesting vector now is shorter than the diameter of the FS. Hence, even through the AF fluctuations are the strongest here, electrons on the FS are hard to pair by $\mathbf{Q_{AF}}$, the system is rather subject to a Mott transition, whose novel features are beyond the scope of this paper.

Fig. 3 displays the inverse pairing susceptibility as a function of temperature, $1/\chi_{pairing}(T)$, at filling $n = 0.9$, $U = 8.5t$, and $N_c = 6$. Here we explicitly project the lattice pairing susceptibility in the s-, $d_{x^2-y^2}$-, and d_{xy}-wave singlet channels and the f-wave triplet channel by using the appropriate form factors. Fig. 3 shows that the two singlet d-wave components are the most divergent ones. Within our numerical resolution their $1/\chi_{pairing}$ extrapolate to zero at the same superconducting transition temperature, T_c. This implies that the superconducting order parameter is doubly degenerate with components $d_{x^2-y^2}$ and d_{xy}. Based on symmetry arguments any linear combination of both d-wave components is possible below T_c. However, both Ginzburg-Landau and BCS-type mean-field approaches favor superconducting phases that break the time-reversal symmetry for singlet multi-component superconductors [31, 32], such as the $d + id$ singlet pairing state predicted in graphene [13, 17] and the cobaltates [12, 14]. Therefore, our findings support the possibility of a chiral $d+id$ superconducting phase in the hole-doped triangular Hubbard model. The inset of Fig. 3 shows the phase diagram for different doping concentrations based on $N_c = 6$ DCA-CTQMC simulations. T_c becomes finite for doping larger than $n = 0.7$ due to the onset of FS nesting and strong AF correlations, and increases as n aproaches 1, reflecting that the AF fluctuations become stronger towards half-filling. However, the nature of the ground state at half-filling is still unclear due to a worsened minus-sign problem in our simulations.

To shine light on the dominant contribution to the pairing interaction, we use the parquet equations to decompose the irreducible particle-particle vertex function, and project each term onto its $d_{x^2-y^2}$ and d_{xy} components. The results are presented in Fig. 4 for a DCA-CTQMC simulation with cluster size $N_c = 12$, $U = 8.5t$ and filling $n = 0.9$. The left, right panels correspond to the d_{xy}, $d_{x^2-y^2}$ projection of the parquet equations, respectively. In both cases, the dominant contribution to the effective pairing interactions $V_{d_{xy}}$ and $V_{d_{x^2-y^2}}$ is from the magnetic, spin $S = 1$, particle-hole channel, $V^S_{d_{xy}}$ and $V^S_{d_{x^2-y^2}}$. In fact, we also find that the pairing interaction, $V_{d_{xy}/d_{x^2-y^2}}(\mathbf{k} - \mathbf{k}')$ is peaked at momen-

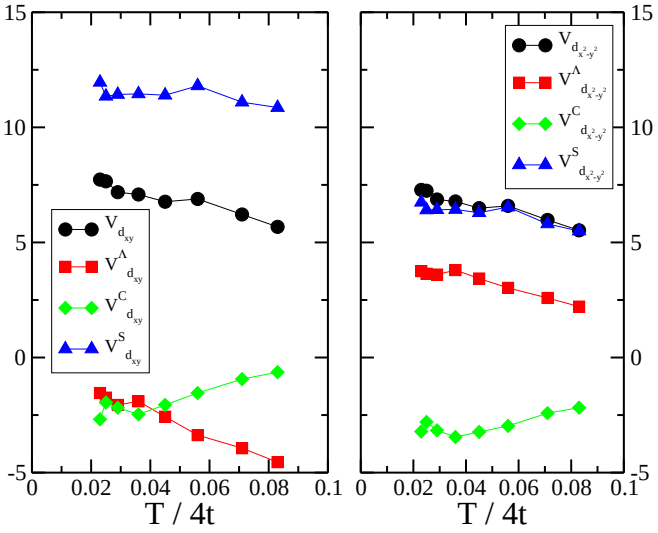

FIG. 4: (Color online) Left: d_{xy} projected contributions to the pairing vertex $V_{d_{xy}}$, from the fully irreducible vertex $V^{\Lambda}_{d_{xy}}$, charge $V^{C}_{d_{xy}}$ and spin $V^{S}_{d_{xy}}$ cross channels versus T at $n = 0.9$, $U = 8.5t$. Right: the $d_{x^2-y^2}$-wave projection of the same quantities. In both cases, the contribution to the pairing interaction from spin channel is clearly dominant.

tum transfer $|\mathbf{k} - \mathbf{k}'| = |\mathbf{Q_{AF}}|$. The vertex decomposition confirms that this peak comes from the spin channel $V^{S}_{d_{xy}/d_{x^2-y^2}}(\mathbf{Q_{AF}})$ (not shown). Note that both $N_c = 6$ and 12 size clusters have the cluster points connected by $\mathbf{Q_{AF}}$. From the BCS gap equation [31]

$$\Delta_{\mathbf{k}} = -\frac{1}{N}\sum_{\mathbf{k}'} V^{SC}(\mathbf{k}-\mathbf{k}')\frac{\Delta_{\mathbf{k}'}}{2E(\mathbf{k}')}\tanh(\frac{E(\mathbf{k}')}{2T}), \quad (2)$$

where $E(\mathbf{k}) = \sqrt{\epsilon^2_{\mathbf{k}} + \Delta^2_{\mathbf{k}}}$, we infer that if the superconducting pairing interaction $V^{SC}(\mathbf{k} - \mathbf{k}')$ is peaked at $\mathbf{Q_{AF}}$, the order parameters $\Delta_{\mathbf{k}}$ which correspond to $d_{x^2-y^2}$, d_{xy} and f-waves are equally favored in the $N_c = 6$ and 12 clusters. Our results suggest that d_{xy} and $d_{x^2-y^2}$ singlet pairing are favored over the f-wave triplet pairing, probably because f-wave has a more complex nodal structure than the two d-waves [1].

Conclusion.- Using large-scale dynamical cluster quantum Monte Carlo simulations, we find a doubly degenerate singlet pairing state at interaction strength close to the bare bandwidth and filling larger than $n = 0.7$ in the hole-doped Hubbard model on the triangular lattice. Our findings suppport the presence of a chiral $d + id$ singlet superconducting phase in this model. The pairing mechanism comes from antiferromagnetic spin fluctuations at the magnetic order wavevector nesting the deformed FS. A decomposition of the vertex further confirms that the spin channel contributes the most to the effective pairing interaction.

We acknowledge G. Chen, K. Kanoda, K.-M. Tam, and Y. Zhou for useful discussions. This work is supported by NSF OISE-0952300 (KSC, JM), and the EPSCoR Cooperative Agreement EPS-1003897 (ZYM). Additional support was provided by the DOE SciDAC grant DE-FC02-10ER25916 (MJ, SXY) and the Korean National Research Foundation Grant NRF-2011-0013866 (UY). Supercomputer support was provided by the NSF XSEDE grant number DMR100007, the Louisiana Optical Network Initiative, and HPC@LSU computing resources.

* Electronic address: kchen5@lsu.edu
† Electronic address: zmeng@lsu.edu

[1] M. Sigrist and K. Ueda, Rev. Mod. Phys. **63**, 239 (1991).
[2] K. Takada, H. Sakurai, E. Takayama-Muromachi, F. Izumi, R. A. Dilanian, and T. Sasaki, Nature **422**, 53 (2003).
[3] R. E. Schaak, T. Klimczuk, M. L. Foo, and R. J. Cava, Nature **424**, 527 (2003).
[4] M. L. Foo, Y. Wang, S. Watauchi, H. W. Zandbergen, T. He, R. J. Cava, and N. P. Ong, Phys. Rev. Lett. **92**, 247001 (2004).
[5] Y. Shimizu, K. Miyagawa, K. Kanoda, M. Maesato, and G. Saito, Phys. Rev. Lett. **91**, 107001 (2003).
[6] Y. Kurosaki, Y. Shimizu, K. Miyagawa, K. Kanoda, and G. Saito, Phys. Rev. Lett. **95**, 177001 (2005).
[7] S. Yamashita, Y. Nakazawa, M. Oguni, Y. Oshima, H. Nojiri, Y. Shimizu, K. Miyagawa, and K. Kanoda, Nat. Phys. **4**, 459 (2008).
[8] M. Yamashita, N. Nakata, Y. Kasahara, T. Sasaki, N. Yoneyama, N. Kobayashi, S. Fujimoto, T. Shibauchi, and Y. Matsuda, Nat. Phys. **5**, 44 (2008).
[9] T. Itou, A. Oyamada, S. Maegawa, M. Tamura, and R. Kato, Phys. Rev. B **77**, 104413 (2008).
[10] S. Yamashita, T. Yamamoto, Y. Nakazawa, M. Tamura, and R. Kato, Nat. Commun **2**, 275 (2011).
[11] P. W. Anderson, Materials Research Bulletin **8**, 153 (1973).
[12] S. Zhou and Z. Wang, Phys. Rev. Lett. **100**, 217002 (2008).
[13] R. Nandkishore, L. S. Levitov, and A. V. Chubukov, Nat. Phys. **8**, 158 (2012).
[14] M. L. Kiesel, C. Platt, W. Hanke, and R. Thomale, arXiv:1301.5662 (2013).
[15] G.-q. Zheng, K. Matano, D. P. Chen, and C. T. Lin, Phys. Rev. B **73**, 180503(R) (2006).
[16] G.-q. Zheng, K. Matano, R.L. Meng, J. Cmaidalka, and C.W. Chu, J. Phys.: Condens. Matter **18**, L63 (2006).
[17] M. L. Kiesel, C. Platt, W. Hanke, D. A. Abanin, and R. Thomale, Phys. Rev. B **86**, 020507(R) (2012).
[18] G. Baskaran, Phys. Rev. Lett. **91**, 097003 (2003).
[19] Q.-H. Wang, D.-H. Lee, and P. A. Lee, Phys. Rev. B **69**, 092504(2004).
[20] Th. Maier, M. Jarrell, T. Pruschke, and M. H. Hettler, Rev. Mod. Phys. **77**, 1027 (2005).
[21] M. H. Hettler, A. N. Tahvildar-Zadeh, M. Jarrell, T. Pruschke, T. and H. R. Krishnamurthy, Phys. Rev. B **58**, R7475 (1998).
[22] A. N. Rubtsov, V. V. Savkin, and A. I. Lichtenstein, Phys. Rev. B **72**, 035122 (2005).

[23] M. Jarrell and J.E. Gubernatis, Phys. Rep. **269**, 133 (1996).
[24] X. Wang, E. Gull, L. Medici, M. Capone, and A. Millis, Phys. Rev. B **80**, 045101 (2009).
[25] K.-S. Chen, Z. Y. Meng, T. Pruschke, J. Moreno, and M. Jarrell, Phys. Rev. B **86**, 165136 (2012).
[26] T.A. Maier, M.S. Jarrell, and D.J. Scalapino, Phys. Rev. Lett. **96**, 047005 (2006).
[27] S.-X. Yang, H. Fotso, S.-Q. Su, D. Galanakis, E. Khatami, J.-H. She, J. Moreno, J. Zannen, and M. Jarrell, Phys. Rev. Lett. **106**, 047004 (2011).
[28] K. Miyake, S. Schmitt-Rink, and C. M. Varma, Phys. Rev. B **34**, 6554(R) (1986).
[29] D. J. Scalapino, E. Loh, Jr., and J. E. Hirsch, Phys. Rev. B **34**, 8190(R) (1986).
[30] C. Honerkamp, Phys Rev. B **68**, 104510 (2003).
[31] R. Joynt and L. Taillefer, Rev. Mod. Phys. **74**, 235 (2002).
[32] V. Kuznetsova and V. Barzykin, Europhysics Letters **72**, 437 (2005).